Optimization of Dilution and Mixing of Biochemical Samples Using Digital Microfluidic Biochips

Sudip Roy, *Student Member, IEEE,* Bhargab B. Bhattacharya, *Fellow, IEEE,* and Krishnendu Chakrabarty, *Fellow, IEEE*

***Abstract*—The recent emergence of lab-on-a-chip (LoC) technology has led to a paradigm shift in many healthcare-related application areas, e.g., point-of-care clinical diagnostics, high-throughput sequencing, and proteomics. A promising category of LoCs is digital microfluidic (DMF)-based biochips, in which nanoliter-volume fluid droplets are manipulated on a 2-D electrode array. A key challenge in designing such chips and mapping lab-bench protocols to a LoC is to carry out the dilution process of biochemical samples efficiently. As an optimization and automation technique, we present a dilution/mixing algorithm that significantly reduces the production of waste droplets. This algorithm takes $O(n)$ time to compute at most n sequential mix/split operations required to achieve any given target concentration with an error in concentration factor less than $\frac{1}{2^n}$. To implement the algorithm, we design an architectural layout of a DMF-based LoC consisting of two $O(n)$-size rotary mixers and $O(n)$ storage electrodes. Simulation results show that the proposed technique always yields nonnegative savings in the number of waste droplets and also in the total number of input droplets compared to earlier methods.**

***Index Terms*—Biochips, computer-aided-design, digital microfluidics (DMFs), dilution of biosamples, mixing algorithms, waste minimization.**

I. Introduction

TO MEET the challenges of healthcare cost for cardiovascular diseases, cancer, diabetes, global HIV crisis, and so on, a new field of interdisciplinary research centered around "lab-on-a-chip (LoC)" is emerging [1]–[5]. Typically, a LoC implements one or more biochemical laboratory protocols or assays on a single chip that is a few square centimeters in size. Research in this new discipline of nanobiotechnology needs the integration of many disciplines, such as microelectronics, biochemistry, *in vitro* diagnostics, computer-aided design and optimization, fabrication technology, and so on. Compared to traditional bench-top procedures, biochips offer the advantages of low sample and reagent consumption, less likelihood of error due to minimal human intervention, high-throughput and high sensitivity [1], [5]–[7]. An ideal on-site biochemical analysis system should be inexpensive, sensitive, fully automated, integrated, and reliable. The emerging application areas include among others, clinical diagnostics, especially the immediate point-of-care diagnosis of diseases, enzymatic analysis (e.g., glucose and lactate assays), deoxyribonucleic acid (DNA) analysis [e.g., polymerase chain reaction (PCR) and nucleic acid sequence analysis], proteomic analysis involving proteins and peptides [4], immunoassay, and environmental toxicity monitoring [8]. Several nontraditional biomedical applications and markets, e.g., immunoassays, clinical chemistry, and high-throughout DNA sequencing, are opening up fundamentally new uses for integrated circuits (ICs).

The worldwide market for *in vitro* diagnostics in 2007 was estimated at $38 billion [9], and 1.5 billion diagnostic tests per year worldwide have been predicted for malaria alone [10]. However, continued growth in this emerging field depends on advances in design automation. In particular, design methods are needed to ensure that LoCs are as versatile as the macrolabs that they are intended to replace. Our paper envisions an automated design flow that will transform LoC research and use, in the same way as design automation revolutionized IC design in the past. This paper is, therefore, especially aligned with the vision of functional diversification and "more than Moore," as articulated in the ITRS 2007 [11], which highlights "medical" as being a "system driver" for the future. Recent years have seen a surge in interest in design automation methods for microfluidic LoC [1], [12]–[24].

The basic idea of a microfluidic biochip is to integrate multiple assay operations, such as detection, sample pretreatment, and sample preparation on one chip [25]. Front-end functions, e.g., dilution control of a sample, can be done on-chip or by preprocessing during sample preparation outside the chip. Since off-chip sample processing and sample preparation pose a significant hindrance to the overall biochemical assay time, for fast and high-throughput applications, sample

Manuscript received January 3, 2010; revised April 26, 2010; accepted June 25, 2010. Date of current version October 20, 2010. The work of S. Roy was supported in part by the Indian Statistical Institute, Kolkata, Indian Institute of Technology Kharagpur, Kharagpur, and in part by the Microsoft India Research Ph.D. Fellowship. The work of K. Chakrabarty was supported in part by the U.S. National Science Foundation, under Grant CCF-0914895. This paper was recommended by Associate Editor Y.-W. Chang.

S. Roy is with the Department of Computer Science and Engineering, Indian Institute of Technology Kharagpur, Kharagpur 721 302, India (e-mail: sudipr@cse.iitkgp.ernet.in).

B. B. Bhattacharya is with the Advanced Computing and Microelectronics Unit, Indian Statistical Institute, Kolkata 700 108, India (e-mail: bhargab@isical.ac.in).

K. Chakrabarty is with the Department of Electrical and Computer Engineering, Duke University, Durham, NC 27708 USA (e-mail: krish@ee.duke.edu).

Color versions of one or more of the figures in this paper are available online at http://ieeexplore.ieee.org.

Digital Object Identifier 10.1109/TCAD.2010.2061790

preprocessing steps should also be automated on-chip, i.e., integrated and self-contained on the biochip itself. The dilution problem arises in numerous biochemical assays for preparation of samples or mixtures, e.g., cDNA for real-time PCR, immunoassays for detecting cytokines in serum samples, which is a marker for inflammation. Several bioassays or protocols to be implemented on digital microfluidic (DMF) biochips, may require any value of concentration [or the dilution factor (DF)] of the samples or reagents. One example of a real assay is enzymatic glucose assay (Trinder's reaction); it uses a DF of 200 or more [26]. Another automated DMF-based protocol for extracting proteins from heterogeneous fluids by precipitation has been explained in [27]. This method requires several reagents with different concentration levels, such as 50 mg/mL of BSA solution (sample), 20% TCA (precipitant), 70/30 v/v chloroform/acetonitrile (rinse solution), and 100 mM borate buffer containing 1% SDS (resolubilizing buffer). It is also needed in quantification of test results using sensors, because the concentration level of the droplet may be beyond the on-chip sensor range.

Dilution is commonly used in biological studies to create a variety of concentrations of the stock solution by mixing it with its diluent on a microfluidic device [28]. Concentrations can extend over a nonlinear or linear range and are generated by two types of dilution methods: serial and linear dilution, respectively. In case of linear dilution, the stock solution and its diluent are mixed in different ratios and can create linearly varying concentrations of the stock solution [29]. On the contrary, in serial dilution, a common example of which is the logarithmic method, a solution is repeatedly diluted using the same mixing ratio, e.g., 1 : 1. Three serial dilutions mixed at 1 : 1 yield concentrations 1/2, 1/4, and 1/8. Thus, the serial dilution method creates discrete nonlinear concentration values of the stock solution [29]. Recently, many dilution devices and schemes have been demonstrated in literature for continuous-flow microfluidics (CMF) [30]–[33], to generate various kinds of mixing or concentration levels in both logarithmic and linear methods. However, in case of DMF-based biochips, biochemical samples can only be mixed using discrete volumes of liquid droplets. Therefore, it is possible to carry out only serial dilution to achieve or approximate desired nonlinear concentration levels. Thus, it is a challenge to achieve a desired concentration of the stock solution within a minimum number of mix/split steps. But, only a few research articles have been reported to date on automatic dilution for the DMF biochips development [26], [34]–[36].

Main results: In this paper, we address the problem of automatic dilution of a sample or mixing of two biochemical reagents using DMF biochips. An open issue in automating dilution with a LoC is to minimize the waste droplets produced in the process, because of the limited availability of stock solutions for samples and costly reagents. To reduce waste, we present here an $O(n)$ time algorithm to compute a sequence of mix/split operations for any given target concentration factor (CF), with an error less than $\frac{1}{2^n}$. Further, to efficiently implement the sequence of droplet mix/split operations, we propose an architectural layout of electrodes consisting of two DMF rotary mixers. This technology will help LoC users to adopt emerging design tools and automation methods.

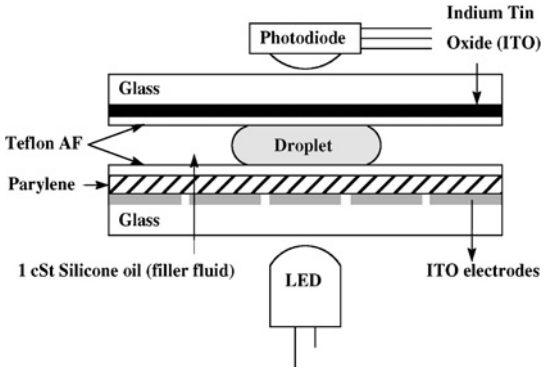

Fig. 1. Schematic of a DMF biochip [1], [7], [39].

The organization of the remainder of this paper is as follows. Section II provides basics of DMF biochips and Section III describes prior related works on automatic dilution and mixing of samples. We present the problem formulation in Section IV. We propose an improved algorithm for diluting a sample that reuses some intermediate concentrations to minimize the wastage in Section V. Simulation results with a comparative study of waste minimization are shown in Section VI. To efficiently implement the sequence of droplet mixing/splitting with a DMF biochip, we propose an architectural layout of electrodes in Section VII. Finally, the conclusion is drawn in Section VIII.

II. Basics of DMF Biochips

In contrast to microarray chips or CMF chips, DMF-based LoCs use electrical actuation to manipulate (transporting, merging, splitting, mixing, dispensing, and so on) discrete droplets of nanoliter volume of the sample or reagent fluids on a 2-D electrode array. Droplet movement is achieved by the modulation of interfacial tension (surface tension) between a conductive fluid and a solid electrode by applying an electric field between them. For liquids with high surface tension, a special phenomenon called electrowetting-on-dielectric effect [37] is observed on DMF biochips [5], [38].

A schematic diagram of the cross-sectional view of a basic cell of a DMF biochip is shown in Fig. 1. Descriptions and architectures of such biochips are available in the literature [7]. A unit cell in the array includes a pair of electrodes that acts as two parallel plates. The bottom plate contains a patterned array of individually controlled electrodes, and the top plate is coated with a continuous ground electrode. The droplet is sandwiched between the two plates and rests on a hydrophobic surface over an electrode. The droplet is moved by applying a control voltage (above a threshold voltage) to an electrode adjacent to the droplet and, at the same time, deactivating the electrode just under the droplet. This electronic method of wettability control creates interfacial tension gradients that move the droplets to the charged electrode. By varying the patterns of control voltage activation, many fluid-handling operations, such as merging, splitting, mixing, and dispensing of droplets, can be executed. In addition to electrodes, optical

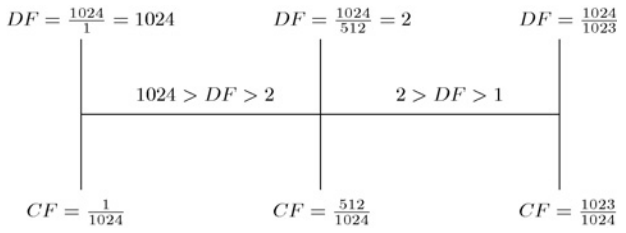

Fig. 2. Correlation between CFs and DFs.

detectors such as light-emitting diodes and photodiodes are also integrated in microfluidic arrays to monitor colorimetric bioassays. In a microfluidic biochip, there are several modules, such as mixers, splitters, detectors, waste reservoirs, dispensers, and so on. Descriptions of a DMF biochip and the four fundamental fluidic operations (dispensing, transporting, mixing, and splitting) have been elaborated elsewhere [1], [40], [41].

III. Prior Art on CAD for Dilution and Mixing with DMF Biochips

A. Mixing Models

DMF biochips typically work with discrete droplets on a uniform 2-D array of equi-sized electrodes, hence, their volumes are always integral multiples of that of a single droplet (unit volume). There are various $(k : \ell)$ mixing models that are often used, where k-unit volume of one substance is mixed with ℓ-unit volume of another substance to produce $(k + \ell)$-unit volume of resultant mixture in a single mixing operation. Three such cases are: 1) $k = \ell = 1$; 2) $k = \ell \neq 1$; and 3) $k \neq \ell$, where k, ℓ are positive integers. The first case, i.e., (1 : 1) mixing model is easy to implement.

B. DF vs. CF

In order to quantify the amount of raw sample (100% conc.) during sample preparation, we will use the terms DF or CF. Both are defined as volume-to-volume ratios and they are related as follows. The DF of a sample can be defined as the ratio of the final volume of the diluted sample (after mixing with the buffer) to the initial volume of the raw sample. The CF is defined as the ratio of the initial volume of the sample to the final volume of the diluted sample (i.e., inverse of the DF, $CF = \frac{1}{DF}$). The DF is always greater than 1 and the CF is always less than 1. This correlation between CF and DF is shown in Fig. 2. The material with which the sample is mixed for dilution is called the diluent or buffer solution, e.g., water or other liquid that is neutral to the sample (i.e., with 0% conc. of sample in it). Thus, dilution is a special case of mixing two substances, where one of them is a buffer (neutral) solution with $CF = 0$. In general, dilution of a sample of CF C_1 can be achieved by mixing it with the same sample of CF C_2, where $C_2 < C_1$. The CF of the resultant sample will lie between C_1 and C_2 because, if the samples of CF C_1 and C_2 are mixed in a volumetric ratio of $k : \ell$, then the resulting sample will have CF $C_r = \frac{k.C_1+\ell.C_2}{k+\ell}$, and a volume of $(k + \ell)$ units.

C. Exponential and Interpolated Dilution

Two basic kinds of dilution are *exponential dilution* and *interpolated dilution*. If a sample is recursively diluted by a buffer solution taking equal volume of both of them for mixing, then the concentration of the sample changes exponentially by a factor of 2, i.e., after n cycles of mixing and balanced splitting, the concentration of the sample changes from C to $\frac{C}{2^n}$, i.e., the DF will be 2^n. This type of dilution is called *exponential dilution*. For example, if two droplets of CFs $\frac{0}{1024}$ and $\frac{1024}{1024}$ are mixed, then the resultant CF becomes $\frac{1}{2}$ (i.e., $DF = 2$). If a sample of concentration C_1 is diluted with its another concentration value C_2 taking equal volume of both of them for mixing, then the final concentration of the sample becomes $\frac{C_1+C_2}{2}$. This is called *interpolated dilution*. For example, if two droplets of CFs $\frac{1022}{1024}$ and $\frac{1024}{1024}$ are mixed, then the resultant CF becomes $\frac{1022+1024}{2.1024}$, i.e., $\frac{1023}{1024}$.

In (1 : 1) mixing model, the simple two-droplet mixing and splitting (into two equal volumetric parts) cycle is deployed repeatedly in order to achieve dilution with a desired target CF. The two constituent substances used at each mix/split cycle are either the supplied sample or buffer solution, or the intermediate droplets produced in the earlier cycles. In each cycle, two unit-volume droplets are produced. The intermediate droplets, which remain unused in the overall dilution process are called waste droplets. Because of the usage of integral volumes of its constituents in mixing, achieving a target CF of a sample in an optimal number of steps with reduction of wastage and storage requirement for intermediate droplets, is a challenge.

D. Prior Art

Several methods of mixing/dilution control techniques for on-chip sample or reagent preparation with DMF biochips have been recently reported [26], [34]–[36]. An experimental study of on-chip dilution control on a layout of electrodes was conducted by Ren *et al.* [26], reporting that 38 integer DFs (in the range 2–64, given the constraint that only 64-fold exponential dilution and 16-fold interpolating dilution were available) can be obtained in ten mix/split cycles by interpolating serial dilution method. In that work, only integer DFs were considered. However, no algorithmic scheme was presented for determining the mixing steps to achieve the target concentration from the initial sample or stock solution.

In order to perform the serial dilution in a systematic manner using a DMF biochip, Griffith *et al.* [34] described an algorithm of time complexity $O(n^3)$ to determine the sequence of mixing/splitting steps, such that the error in the CF is less than $\frac{1}{2^n}$. The procedure can be completed in at most n (1 : 1) sequential mix/split steps assuming that multiple droplets of intermediate CFs are available as needed. A binary search strategy was used to determine the intermediate concentration levels of the droplets to be mixed. However, the design of a suitable architectural layout of electrodes for efficient implementation of the above-mentioned algorithm was left as an open problem. The layout should be capable of supplying all the required number of droplets of intermediate CF as demanded by the dilution process. Another open issue is to

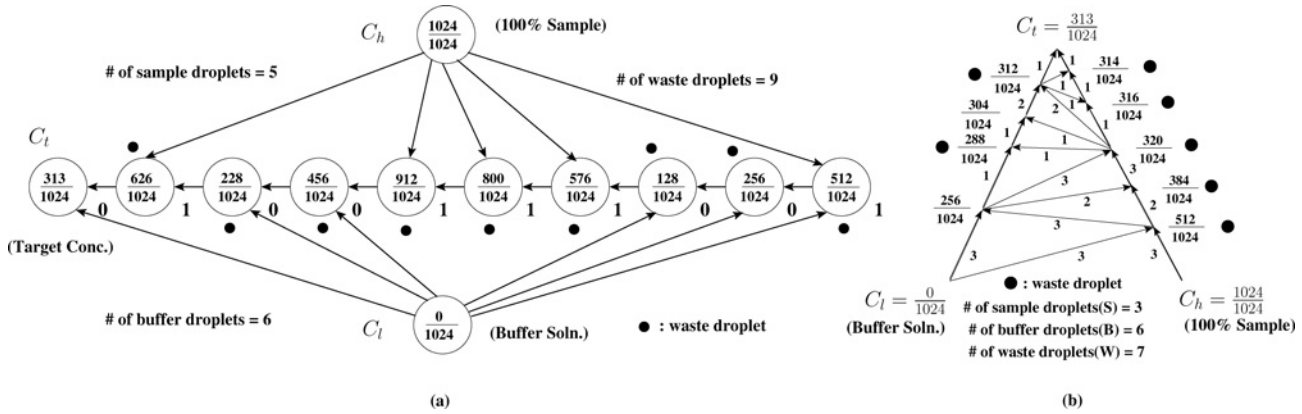

Fig. 3. Mix/split steps for target $C_t = \frac{313}{1024}$ ($\equiv 0.0100111001_2$). (a) BS method [36]. (b) Proposed scheme.

resolve the problem of managing the storage and reuse of these intermediate droplets.

Recently, a mixing/dilution algorithm based on bit-scanning (BS) method has been proposed by Thies *et al.* [36] for mixing two or more fluids (sample/reagent) at any given ratio considering (1 : 1) mixing model. Given the desired ratio of the two (or more) constituents, it converts the target CFs into their binary representations and then scans the bits from right-to-left to decide upon the mixing and splitting steps [Fig. 3(a)]. For mixing two fluids (e.g., dilution purposes) this method has the advantage that no storage of droplets with earlier intermediate CFs is required; only the current droplet along with the initial sample or the buffer is required for the next step. However, none of the above methods focused on wastage control and, currently, there exists no such on-chip waste minimizing dilution control scheme for such biochips. Another important practical issue is stated as an open problem [36]; if two inputs are related (e.g., a sample of 10% acid and a sample of 20% of the same acid), then how to produce an intermediate CF of the sample (say, 17% acid) using them. Again, no architectural layout of electrodes was suggested for executing the mixing/dilution scheme on-chip, and, therefore, the related design problem needs to be addressed.

IV. Problem Formulation

The problem of dilution can be stated as follows. Given the supply of a sample or reagent (with 100% conc.) and a neutral buffer solution (0% conc.), determine a sequence of $(k : k)$ mix/split steps for obtaining a droplet with a desired target CF of the sample. In a more generalized version of the problem, the sample is supplied with two arbitrary CFs, one lower (C_l), and one higher (C_h) than the target CF, and the goal is to determine the mix/split sequence to produce the target sample. For a neutral buffer solution, $C_l = 0$. There are four important issues to be resolved in executing the dilution process: 1) developing an efficient algorithm for determining the mix/split sequence; 2) minimization of the length of the sequence, i.e., actual on-chip dilution time in order to achieve a certain precision of CF; 3) reduction of the number of waste droplets for producing a given number of target droplets; and 4) designing a suitable LoC architecture that supports the above objectives efficiently on-chip.

In (1 : 1) mixing model as defined earlier, mixing of two unit-volume droplets of CFs, X and Y [denoted as $mix(X, Y)$], yields a mixture of $CF = \frac{X+Y}{2}$. Thus, to limit the error in target CF C_t by $\frac{1}{2^n}$, one needs a sequence of at most n mix/split steps. So, for the convenience of executing a dilution algorithm, each CF value, which always lies within 0 and 1, is approximated as a rational number with 2^n in the denominator.

The dilution problem can now be formally stated as follows.

1) *Input:* Given a sample with two CFs, C_l and C_h, and the target CF as C_t, such that $0\% \leq C_l < C_t < C_h \leq 100\%$, the maximum number of sequential mix/split steps is n.
2) *Output:* M, a sequence of mix/split steps to achieve C_t starting from C_l and C_h, i.e., $M = m_1, m_2, \cdots, m_n$, where $m_i = mix\_split(X_i, Y_i)$ and X_i, Y_i are the earlier intermediate CFs including the two given input CFs, C_l and C_h.

Let W be the total number of waste droplets produced in the dilution process to achieve a target CF, and let S and B be the total number of droplets of sample and buffer solution, respectively, required to complete the above dilution process.

V. Proposed Dilution Algorithm

A. Algorithm Overview

The proposed algorithm for dilution and mixing with reduced wastage (DMRW) proceeds as follows. It starts with the two initial CFs. At every mix/split step, the algorithm requires only two CFs, called the boundary CFs, one lower and one higher than the target C_t among those CFs already generated, such that the interval between the boundary CFs is minimum. It is easy to verify that this interval is uniquely defined. After mixing the two boundary samples at any instant of time, it checks whether the resulting CF is less or greater than C_t; in the former case, this current sample is mixed with the sample having the smallest CF greater than it and in the latter case, it is mixed with the largest CF sample smaller than it. In this process, the resulting CF approaches further toward C_t.

To repeat this process systematically, in the first case, the lower boundary of CF is changed to the current CF keeping

the higher boundary CF same as the previous one, and in the second case, where the current concentration is greater than C_t, the higher boundary CF is changes to the current CF keeping the lower boundary CF same as the previous one. One important point to be noted here is the fact that at any instant of time, only the droplets with the two current boundary CFs are needed to generate the next droplet. This mix/split process continues until the target concentration C_t reaches the error bound. The sequence can be conveniently depicted using a *mix/split directed graph (digraph)* as shown in Fig. 3(b). The mix/split sequence starting from the two initial boundary CFs through various intermediate CFs to the target C_t is represented by the longest directed path in the digraph. In the digraph, the values of CFs corresponding to the nodes on the left side (right side) increase (decrease) in the direction toward the target node of CF C_t. The algorithm DMRW terminates within n mix/split steps, because the interval between the two current boundary CFs, which includes the target C_t, becomes half of the just preceding interval at each mix/split step. Thus, after at most n sequential steps, the absolute value of the error becomes less than $\frac{1}{2^n}$.

Our algorithm has a backtracing phase that determines the number of intermediate droplets of earlier CFs needed for generating the required number of droplets with the current CF. By performing this backtracing phase from the target CF toward the two initial CFs, the demands for all intermediate CFs and those for the initial CFs, are determined. The proposed scheme is formally described as algorithm DMRW.

Algorithm 1 DMRW (C_l, C_h, C_t)

1: Represent C_l and C_h by rational numbers $\frac{a}{2^n}$ and $\frac{b}{2^n}$, respectively, for some n (number of mix/split steps, i.e., precision level); a, b, n are integers and $0 \leq a < b \leq 2^n$.
2: Approximate the desired $CF = C_t$ as a rational number $\frac{c}{2^n}$, where $0 \leq a < c < b \leq 2^n$; c is an integer.
3: Let the largest (smallest) CF smaller (larger) than C_t be $\frac{L}{2^n}\left(\frac{R}{2^n}\right)$, where initially, $L = a$ and $R = b$. These values represent the two boundary CFs, which appear as the highest node on the left arm and on the right arm of the digraph respectively, at any instant of time.
4: Mix a unit-volume droplet of $CF = \frac{L}{2^n}$ with that of $CF = \frac{R}{2^n}$ to obtain a two-unit volume droplet of $CF = X = \frac{x}{2^n}$, where $x = \frac{L+R}{2}$; Calculate *error* in CF as $|X - C_t|$.
5: **while** $error \geq \frac{1}{2^n}$ **do**
6: **if** $x < c$ **then**
7: Set $L = x$.
8: **else**
9: Set $R = x$.
10: **end if**
11: $mix\_split\left(\frac{L}{2^n}, \frac{R}{2^n}\right)$, i.e., mix two unit-volume droplets of CFs $\frac{L}{2^n}$ and $\frac{R}{2^n}$, and split into two unit-volume droplets of with current $CF = X$; $NumOfSteps = NumOfSteps + 1$.
12: Calculate $error = |X - C_t|$.
13: **end while**
14: Obtain the current droplet with desired CF $C_t = X \simeq \frac{c}{2^n}$.
15: Backtrace the pointers of the mix/split digraph from the target CF C_t to the start in order to determine the required number of droplets with intermediate values of CF and the number of supplied droplets as demanded during the target droplet(s) generation process.

B. Example

An example of generating droplets of target concentration $C_t = \frac{313}{1024} \simeq 0.30566_{10} \equiv 0.0100111001_2$ using the BS method [36] is shown in Fig. 3(a). This method works only when the initial volumes are given with $CF = 0$ (buffer) and $CF = 1$ (100% conc.) sample. It may be observed that the number of 1s in the n-bit binary representation of C_t (here, it is five) indicates the total number of sample droplets required, whereas, the number of 0s plus one (ignoring all the 0s on the right of the least significant 1 bit position) indicates the total number of buffer droplets required (here, it is six). Here, the number of mixing/splitting steps required to get the target droplet is ten and the total number of waste droplets in the process is the number of mix/split steps excluding the last one, or in other words, is equal to the length of binary string minus one (here, it is nine). In contrast, an example of obtaining the target CF $C_t = \frac{313}{1024}$ using the proposed algorithm is shown in Fig. 3(b). The mix/split steps obtained from this digraph are shown in Table III.

C. Backtracing in the Digraph

By backtracing from the target C_t toward the initial two boundary CFs, the numbers of droplets required to produce each intermediate concentration are calculated, which are shown as labels of directed edges of the graph. Fig. 4 shows the steps of backtracing in the mix/split digraph starting from the target CF toward the two input CFs for the target CF $C_t = \frac{313}{1024}$. The pattern of droplet demand for the nodes in the mix/split digraph is shown in Fig. 3(b) and in Table IV. Here, it is easy to check that the total numbers of sample and buffer droplets required are three and six, respectively, while there are only seven waste droplets lost during the production of two target droplets after ten mix/split steps. Simulation results reported later demonstrate that the proposed method provides a significant amount of savings in sample/buffer consumption.

D. Example of Generalized Dilution

An example showing how a target CF is achieved using two different CFs other than the raw sample or reagent (with 100% conc.) and a neutral buffer solution (0% conc.), is illustrated in Fig. 5. Let us assume that given $C_l = \frac{13}{1024}$ and $C_h = \frac{1011}{1024}$, we need to generate a target with $C_t = \frac{89}{1024}$ with at most ten mix/split steps. The mix/split digraph as shown in Fig. 5 reveals that the target CF can be achieved in nine mix/split steps, which produce five unit-volume waste droplets.

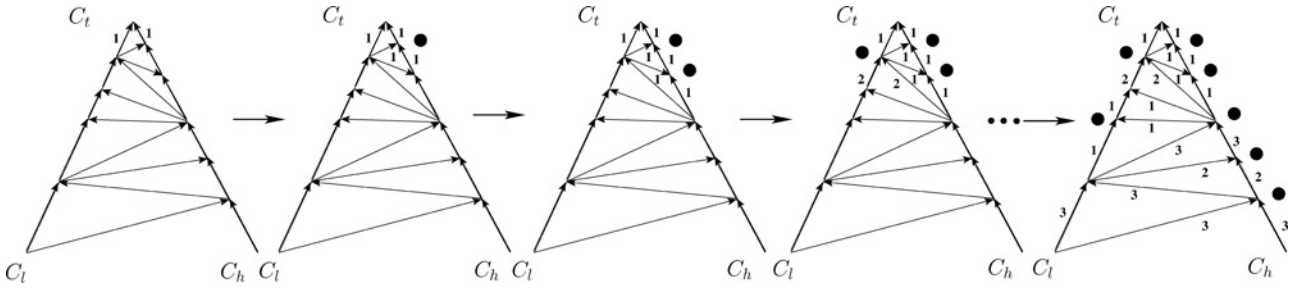

Fig. 4. Steps of backtracing of the mix/split digraph for target CF $C_t = \frac{313}{1024}$.

E. Design Complexity Issues

An on-chip mix/split module fed with two droplets produces only two droplets after splitting. The above method of dilution may require more than two droplets of the current two boundary CFs, at different steps of the dilution process. For example, as seen from Fig. 3(b), in order to produce target $C_t = \frac{313}{1024}$, we need four droplets of intermediate $CF = \frac{320}{1024}$, and five droplets of $CF = \frac{256}{1024}$. Thus, if such a simple mixer/splitter module is used, in order to meet the multiple droplet demand of such intermediate CFs, the dilution process may need to be initiated right from the beginning to supply the intermediate droplets when required again. To alleviate this problem, the last step of assessing demands of droplets is included in our algorithm, which provides a measure of demand and consequent supply of all the boundary droplets in course of the entire dilution process. This information also leads to an efficient design of a chip architecture, described later in this paper, with only two DMF rotary mixers and two storage areas with space complexity $O(n)$ for an accuracy of $\frac{1}{2^n}$, i.e., the resultant CF in the last mix/split step should have an error in target CF less than $\frac{1}{2^n}$. Such a design not only expedites the dilution process but also reduces the wastage to a significant extent. It may be noted in this context, that in the BS method [36], as illustrated in Fig. 3(a), in every mix/split step, exactly one droplet of each of the two constituents is needed, and consequently, the wastage is constant (i.e., $n-1$). The proposed algorithm for determining the sequence of mix-split steps to achieve dilution of a sample is of time complexity $O(n)$ as we need to use only the two current boundary CFs; the CF of the resulting droplet is the mean value of those of its two constituents, where n is the number of bits in the binary expression of the desired target CF.

In contrast, the previous algorithm proposed in [34] examines exhaustively all previously explored CFs to decide upon the current best pair of CFs to be used in the mixing process iteratively, with an ultimate goal of achieving the desired target concentration of the sample. This is done by pairwise comparison between all the intermediate concentration levels; for n digits of precision, the progress toward the target continues akin to a binary search method, and the above pairwise comparison is repeated $O(n)$ times. Thus, the worst-case time complexity of the earlier scheme [34] of mix/split sequence determination is $O(n^3)$, although, after the mix-split sequence is determined, the actual on-chip dilution process can be performed in $O(n)$ mix/split steps for producing the target droplet. It may be noted that the proposed method uses only the two current boundary CFs in each mix-split operation, in contrast to the exhaustive search of the earlier scheme [34].

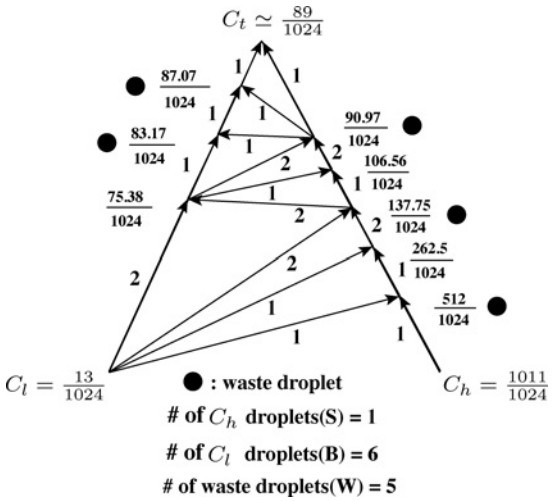

Fig. 5. Mix/split steps for target $C_t = \frac{89}{1024}$, using droplets with CFs $C_l = \frac{13}{1024}$ and $C_h = \frac{1011}{1024}$.

The following discussion elaborates the similarities and differences between the proposed method DMRW and the dilution algorithm proposed by Griffith *et al.* [34]. Both algorithms produce the target CF with the same accuracy within n mix/split steps. Since at each mix/split step, the resultant CF becomes half of the sum of its two constituent CFs, the error that can occur after n mix/split steps is less than $\frac{1}{2^n}$. Hence, the quality of the solutions obtained by both the methods is the same. As described earlier, the computation time for determining the n mix/split steps for a target CF is more in the case of the dilution algorithm of Griffith *et al.* [34] compared to our proposed algorithm DMRW. The problem of waste minimization was not addressed earlier and no architectural layout of electrodes to support on-chip dilution of a sample was addressed either [34], [36]. The proposed DMRW algorithm admits an efficient layout of electrodes on-chip, which is presented in this paper later. Furthermore, in the method of Griffith *et al.* [34], the use of intermediate CFs is decided by checking all the previously generated droplets at every step of the algorithm. Hence, proper management of droplet storage is hard, which, in turn, complicates on-chip dilution process.

The above discussion leads to the following observation.

The proposed algorithm DMRW always produces a target mixture with CF C_t with an error less than $\frac{1}{2^n}$, given the two input CFs C_l and C_h of the sample fluid ($0 \leq C_l < C_t < C_h \leq 1$), in at most n sequential mix/split steps.

Theorem 1: In DMRW, for each of the target CFs with a desired accuracy, a nonnegative savings will be observed in the number of waste droplets in comparison with the BS method.

Proof: In the last (1 : 1) mixing step, two unit-volume target droplets are produced. At any earlier step, if the droplet demand of an intermediate CF is an even number, say $2p$, then the demand of each its two constituents will be p. Thus, either (1 : 1) mix/split steps are to be repeated p times, or one (p : p) mix step is required. On the other hand, when the required demand is odd, say $2p+1$, then at least $2p+2$ droplets should have to be produced, in (k : k) mix/split model. Hence, at each mix/split node of the digraph that reflects the execution trace of DMRW, at most one waste droplet can be produced, because otherwise, fewer constituent droplets would have been required over all repeated operations of this mix/split step.

Let W_1 denote the total number of waste droplets produced by algorithm DMRW. If k_1 mix/split nodes appear in the digraph, ($k_1 \leq n$), for a given target CF, then $W_1 \leq (k_1 - 1)$, because for some of the mix/split nodes, the number of waste droplets may be zero.

Let W_2 denote the total number of waste droplets produced by the BS method. If it executes k_2 mix/split steps ($k_2 \leq n$) for a given target CF, then there will be exactly $(k_2 - 1)$ waste droplets, i.e., $W_2 = k_2 - 1$. Since for the same accuracy level, $k_1 = k_2$, $W_1 \leq W_2$. ■

Theorem 2: For dilution of a sample, there will always be a nonnegative savings in the total number of required input droplets when DMRW is run, compared to the BS method.

Proof: We prove this result by contradiction. In order to produce a diluted sample by mixing it with a buffer, let the required number of sample and buffer be S and B, respectively. If we need the same number t of target droplets, then for both DMRW and BS methods, the relation is immediate as follows:

$$S + B = W + t \tag{1}$$

where $t \geq 2$ is an even number, because if the same mix/split sequence is repeated, then at the end of each pass, two target droplets are obtained.

So

$$\begin{aligned} S_1 + B_1 &= W_1 + t \ (DMRW) \\ S_2 + B_2 &= W_2 + t \ (BS \ method). \end{aligned}$$

For a given target CF C_t, $W_1 \leq W_2$ holds.

Therefore, $(S_1 + B_1) \leq (S_2 + B_2)$.

Hence, if $S_1 > S_2$, then $B_1 < B_2$, and if $B_1 > B_2$, then $S_1 < S_2$. Again, if $(S_1 + B_1) > (S_2 + B_2)$, then the savings in waste obtained by running DMRW will be negative, i.e., $W_1 > W_2$, which is a contradiction. ■

VI. Simulation Results

The simulation results of the proposed algorithm DMRW for $n = 10$ are reported in this section. We have simulated both the proposed scheme and the BS method [36] for various target CFs in the range of $\frac{1}{1024}$ to $\frac{1023}{1024}$. We calculate the percentage savings in sample/buffer solution consumption or in wastage as follows:

$$\frac{D_1 - D_2}{D_1} \times 100\% \tag{2}$$

where D_1 is the number of droplets of the fluid (sample, buffer, or waste) in the BS method and D_2 is the number of droplets of the corresponding fluid in the proposed method DMRW. We also compute y for each percentage value x, where y is the number of target CFs with $x\%$ savings in number of droplets, for sample, buffer, or waste. The plots of y against x (i.e., the histograms) are shown in Fig. 6.

We have observed significant (always nonnegative) savings in the number of waste droplets while generating the target CF using a maximum of ten mix/split cycles by the proposed method. This, in turn, leads to savings in the consumption of sample/reagent and of buffer solution in most of the cases. Simulation data for some of the target CFs are listed in Table I with two initial CFs as 0% conc. and 100% conc., including the percentage savings in the number of sample, buffer, and waste droplets compared to the BS method [36].

We observed that there are 121 CF values within the range $\frac{1}{1024}$–$\frac{1023}{1024}$, which produce negative savings either in buffer solution or in sample fluid, i.e., for them the consumption of either sample or buffer is more than those cases for the method of [36] (such as for CFs $\frac{127}{1024}$, $\frac{511}{1024}$, $\frac{513}{1024}$, and $\frac{897}{1024}$). However, for the remaining 902 CF values, we observe nonnegative savings in sample/buffer consumption. In Table I, we provide comparison of number of droplets of sample, buffer, and waste fluids for four such CFs ($\frac{127}{1024}$, $\frac{511}{1024}$, $\frac{513}{1024}$, and $\frac{897}{1024}$) for which the percentage savings of either sample or buffer are negative.

Let us consider three extreme cases of target CFs: $\frac{127}{1024}$, $\frac{341}{1024}$, and $\frac{513}{1024}$ using $\frac{0}{1024}$ and $\frac{1024}{1024}$ as the two input CFs. The mix/split digraphs for the target CFs $\frac{127}{1024}$, $\frac{341}{1024}$, and $\frac{513}{1024}$ are shown in Fig. 7(a)–(c), respectively. For the target $CF = \frac{127}{1024} \equiv 0.0001111111_2$, the number of sample (buffer) droplets required in the BS method is seven (four), and nine waste droplets are produced. On executing the proposed method, they are observed to be one, eight, and seven, respectively. Thus, a savings of (85.7%) in sample fluid is observed. In the case of the target $CF = \frac{341}{1024} \equiv 0.0101010101_2$, the number of sample (buffer) droplets required in the BS method is five (six), and nine waste droplets are produced. In the proposed method, they are one, two, and one, respectively, and thus a savings of (88.9%) in waste droplets is observed. From the binary representation of $CF = \frac{513}{1024} \equiv 0.1000000001_2$, it follows that the number of sample (buffer) droplets required in the BS method is two (nine), and nine waste droplets are produced. In the proposed method, they are six (five) and nine, respectively. Thus, a negative savings in sample consumption is observed by the proposed method DMRW. However, the total input demand (sample + buffer) remains the same for both the methods.

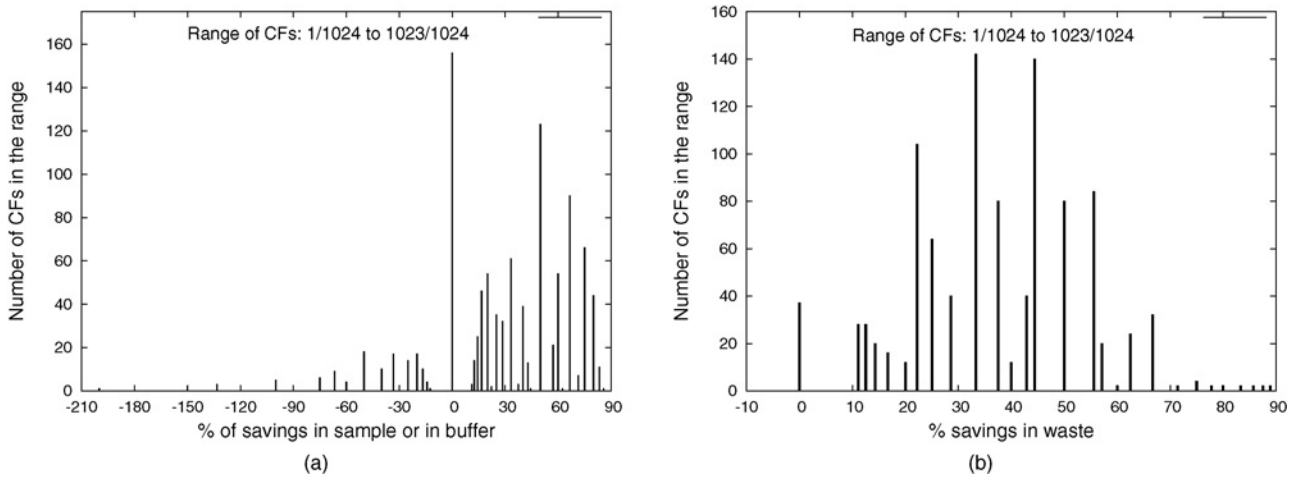

Fig. 6. Histogram of CFs with various percentage savings in the number of droplets. (a) Sample or buffer solution. (b) Waste fluid.

TABLE I

SAVINGS IN THE NUMBER OF DROPLETS FOR SOME EXAMPLE CFS USING THE PROPOSED SCHEME

CF (≡binary)	# of Droplets of Total Input (Sample + Buffer)	# of Waste Droplets	% Savings in Total Input (Sample + Buffer)	% Savings in Waste
51/1024 ($\equiv 0.0000110011_2$)	7 (11)	5 (9)	36.4	44.4
127/1024 ($\equiv 0.0001111111_2$)	9 (11)	7 (9)	18.2	22.2
205/1024 ($\equiv 0.0011001101_2$)	5 (11)	3 (9)	54.5	66.7
313/1024 ($\equiv 0.0100111001_2$)	9 (11)	7 (9)	18.2	22.2
341/1024 ($\equiv 0.0101010101_2$)	3 (11)	1 (9)	72.7	88.9
511/1024 ($\equiv 0.0111111111_2$)	11 (11)	9 (9)	0	0
512/1024 ($\equiv 0.1_2$)	2 (2)	0 (0)	0	0
513/1024 ($\equiv 0.1000000001_2$)	11 (11)	9 (9)	0	0
897/1024 ($\equiv 0.1110000001_2$)	9 (11)	7 (9)	18.2	22.2

Numbers within "( )" corresponds to the BS method [36].

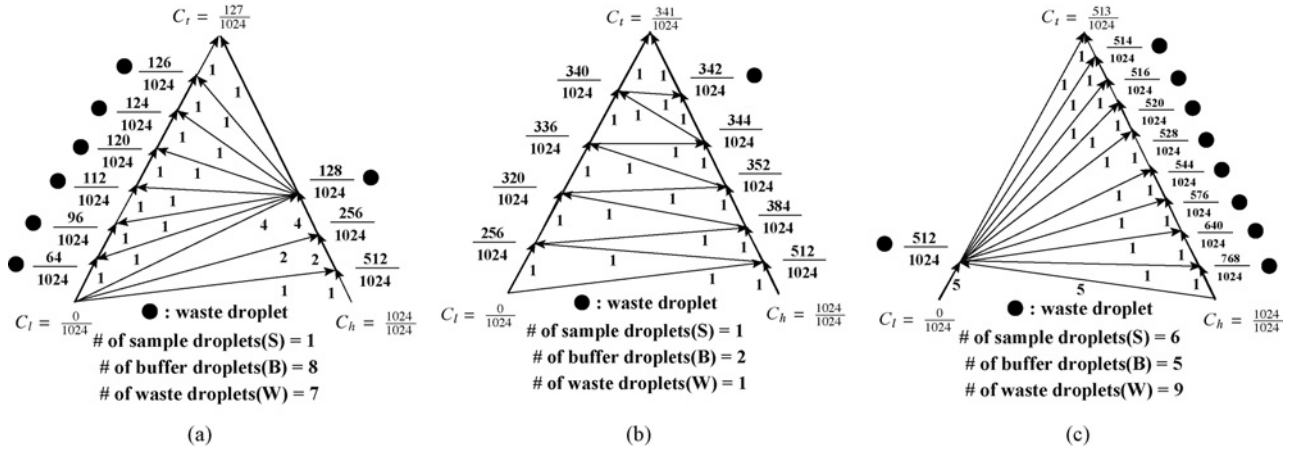

Fig. 7. Mix/split steps obtained by the proposed scheme for the target CF. (a) $C_t = \frac{127}{1024}$. (b) $C_t = \frac{341}{1024}$. (c) $C_t = \frac{513}{1024}$.

TABLE II
SAVINGS IN THE NUMBER OF DROPLETS COMPARED TO THE BS METHOD [36]

Sample/Reagent	Max. Savings	85.7%
	Avg. Savings	29%
Buffer Solution	Max. Savings	85.7%
	Avg. Savings	29%
Waste	Max. Savings	88.9%
	Avg. Savings	36.8%

It is shown earlier theoretically that DMRW algorithm never increases waste droplet production or the total input demand. Reducing the number of waste and input droplets is important for several reasons. For instance, there can only be a limited number of waste reservoirs on-chip or the reservoir capacity to hold samples, reagents, or buffers may be limited. There is a critical practical constraint of limited volume of these stock solutions [42], [43]. Furthermore, transportation of input or waste droplets adds to droplet routing complexity, which leads to increased power consumption. Hence, the proposed scheme is suitable for waste-aware dilution management provided an appropriate on-chip layout architecture is designed to support the scheme.

Experimental results reveal that for most of the cases, it reduces wastage compared to the BS method (for 986 target CFs out of 1023 CFs, i.e., for 96% cases). Again, in the case of 746 target CFs out of 1023 CFs, the proposed algorithm reduces the sample fluid consumption (i.e., for 73% cases) and for 156 target CFs, it consumes the same amount of sample fluid compared to the BS method. Thus, for 902 target CFs, our algorithm does not need more sample consumption compared to the earlier method of [36] (i.e., for 88% cases).

The histograms of CFs between $\frac{1}{1024}$ and $\frac{1023}{1024}$ against average percentage savings in the number of sample or buffer solution and waste droplets are shown in Fig. 6(a) and (b), respectively.

Within the range of CFs from $\frac{1}{1024}$ to $\frac{1023}{1024}$, the simulation results have been summarized in Table II, which shows percentage savings in sample and buffer usage and percentage savings in waste droplets by the proposed scheme compared to [36].

Observation 1*:* Over the range of CFs from $\frac{1}{1024}$ to $\frac{1023}{1024}$, if C_{t1} is a target CF, for which perce ntage savings in sample is x and in buffer is y, then there exists another target CF C_{t2}, for which percentage savings in sample will be y and that in buffer will be x. These two target CFs C_{t1} and C_{t2} are related as follows: $C_{t2} = 1 - C_{t1}$, which is evident if we interchange the sample and buffer nodes in the mix/split digraph of the target CF C_{t1}. For these two target CFs, C_{t1} and C_{t2}, the waste savings will be the same, since the total input demand remains the same. Thus, over the full range of the target CFs, for each of the percentage saving values for the sample, there are the same number of CFs with same percentage saving values for the buffer solution. Hence, the histogram of CFs for sample savings will be identical to that of CFs for similar buffer savings.

As observed earlier, the DMRW method may require multiple droplets of boundary CFs. To achieve an error bound of $\frac{1}{2^n}$ in target CF, one can either use at most n (k:k) mix/split steps, where $k = \lceil \frac{n-1}{2} \rceil$, or one can use purely (1:1) mix/split steps. In the former case, an appropriate (k:k) mixer is to be designed. In the latter case, the total number of (1:1) mix/split operations will increase in comparison to that of BS method [36]. To demonstrate this, we simulate both the DMRW and the BS method over the range of target CFs from $\frac{1}{1024}$ to $\frac{1023}{1024}$, and the (1:1)-mixing steps for each target CF have been counted. The histograms of the CFs with respect to the number of (1:1) mix/split steps are shown in Fig. 8.

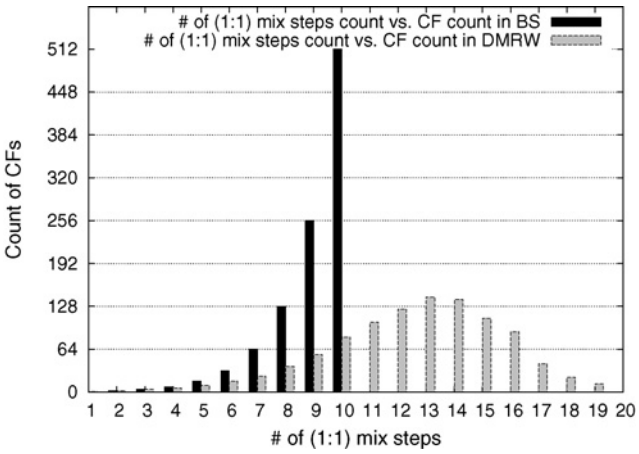

Fig. 8. Histogram of CF counts of CFs with respect to the number of (1 : 1) mixing steps in BS and DMRW methods for $n = 10$.

It is observed that several target CFs in the DMRW method requires more than ten (1:1) mix/split steps, whereas the BS method never needs more than ten (1:1) mixing steps. For instance, to achieve $C_t = \frac{127}{1024}$ using DMRW method, one requires eight (1:1), one (2:2), and one (4 : 4) mix/split steps, i.e., a total of ten steps under (k:k) mixing model, or equivalently, 14 (1:1) mix/split steps [see Fig. 7(a)]. Thus, a suitable architectural layout to support (k:k) mixing model is needed for efficient implementation of DMRW algorithm.

VII. PROPOSED LAYOUTS FOR DMRW ALGORITHM

As evident from the statistics depicted in Fig. 8, on-chip implementation of DMRW algorithm using (1 : 1) mixers will increase the dilution time compared to that for the BS method. To address the multiplicity of droplet demand, it may be faster and useful if the droplets of two boundary CFs are mixed in equal proportions (k : k), $k \geq 1$, in one mixing operation. For example, as shown in Fig. 3(b), three droplets of the sample and three droplets of the buffer solution can be mixed initially at the same time to produce six unit-volume droplets with $CF = \frac{512}{1024}$, to meet the demand for five droplets. Similarly, three droplets with $CF = \frac{384}{1024}$ and three droplets with $CF = \frac{256}{1024}$ can be mixed concurrently to obtain six unit-volume droplets with $CF = \frac{320}{1024}$. It is easy to observe that the total number of droplets of sample or buffer demanded at any stage may be at most $(n-1)$, where $\frac{1}{2^n}$ is the desired accuracy of the target concentration. For example, to obtain a target CF $C_t = \frac{1}{1024}$, the number of droplets required for sample (with 100% conc.) is one and that for the buffer solution (with 0% conc.) is nine, while to obtain a target CF $C_t = \frac{1023}{1024}$, the

number of droplets required for sample (with 100% conc.) is nine and that for the buffer solution (with 0% conc.) is one.

Since the maximum demand of droplets for a boundary CF is $(n-1)$, to generate droplets from its two constituent CFs, $\lceil \frac{n-1}{2} \rceil$ droplets of the two constituents, each, are to be mixed. For example, to obtain nine droplets of $CF = \frac{512}{1024}$ (if the target CF is $\frac{513}{1024}$), five droplets of $CF = \frac{1024}{1024}$ and five droplets of $CF = \frac{0}{1024}$ can be mixed in one step. Then, these droplets (here, nine droplets of $CF = \frac{512}{1024}$) can be used in the subsequent steps of mix/split as needed [see Fig. 7(c)]. Thus, to achieve an accuracy of $\frac{1}{2^n}$ in target CF with at most n $(k : k)$ mixing steps, $k \leq \lceil \frac{n-1}{2} \rceil$. Hence, an array mixer for mixing two samples each with $\lceil \frac{n-1}{2} \rceil$ droplets can be used for this purpose to mix them in one step. However, dispensing of the droplets from the mixer as needed, would again require a sequence of balanced splitting. This, in turn, would require more mixer/splitter modules and the process would be inherently slow, thereby increasing the delay in the dilution process.

A. Design of DMF Rotary Mixer

To circumvent the above problem, we propose to use a DMF rotary mixer, which not only serves as a general purpose $(k : k)$-mixer, $1 \leq k \leq \lceil \frac{n-1}{2} \rceil$, but also allows loading and unloading of droplets one-by-one. In a DMF rotary mixer, multiple electrodes of trapezoidal shape (rather than squared shape of array of electrodes in the layout) are arranged in a circular manner. Instead of executing k $(1 : 1)$ mix/split steps sequentially, we can implement it in one step by using a $(k : k)$ DMF rotary mixer to produce $2k$ droplets of target CF. Implementation of DMF rotary mixers has been demonstrated earlier [44]. The droplets in a rotary mixer can move through adjacent electrodes in the same fashion as that on an array of adjacent electrodes by applying voltages to the electrodes.

A maximum of ten mix/split steps can provide a good approximation to a target CF with a maximum error in the CF of $\frac{1}{2^{10}} \simeq 0.0009765625$, which is very small. Also, the volumetric error of the droplets (during dispensing and splitting of them) increases with the number of dilution cycles (mixing and splitting) required [26]. So, we restrict our architectural design of layout of electrodes for $n \leq 10$. For a dilution process with a maximum of ten mix/split steps, at most total ten-unit volume of fluid (sample + buffer) is mixed at a time. So, along with the ten electrodes, another six electrodes are laid while designing a DMF rotary mixer. These electrodes will aid free movement or rotational stirring of the fluid in order to achieve faster and homogeneous mixing. Thus, the DMF rotary mixer needs at least 16 electrodes with any two neighboring electrodes making an angle of 22.5° at the center Fig. 9. In general, the size of the DMF rotary mixer can be of $(2.\lceil \frac{n-1}{2} \rceil + 6)$ electrodes, for a precision of up to n-bit binary representation of the target CF. The dispensing of droplets, one at a time, from the DMF rotary mixer is illustrated in Fig. 9. The actuation sequence represents the logic values (1 or 0) of the voltages (high or low) applied to the 16 addressed electrodes with the clock cycles. In this figure, it is shown how a unit-volume droplet can be dispensed from a mixture of three-unit volume droplets by applying splitting forces in orthogonal directions.

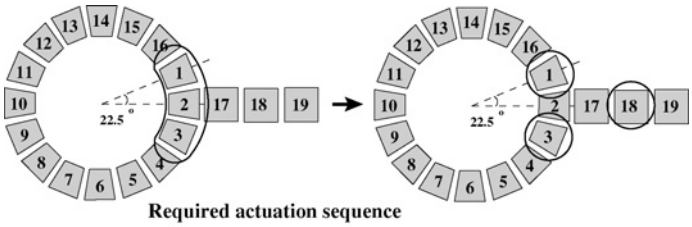

Required actuation sequence

Clock Cycle	16	1	2	3	4	17	18	19
0	0	1	1	1	0	0	0	0
1	0	1	0	1	0	1	1	0
2	0	1	0	1	0	0	1	0

Fig. 9. Dispensing one unit-volume droplet from a DMF rotary mixer of 16 electrodes having three-unit volume droplets (electrodes 5–15 can be kept at logic 1 or 0).

It has been experimentally observed that, while dispensing one unit-volume droplet in the above case, both the electrode 17 and 18 are needed to be simultaneously applied high voltages for one clock cycle to produce a pull or drag force to bring out that droplet from the three-unit volume fluid. Also, the middle electrode (electrode number 17) should be made logic 0 in the next clock cycle, so that the droplet on electrode 18 does not mix with the fluid in the DMF rotary mixer. Thus, this mechanism of droplet dispensing from the DMF rotary mixer avoids unintended mixing. Further, the total number of droplets demanded at any instant is $(n-1)$, each of which can be dispensed one-by-one from the DMF rotary mixer using the mechanism shown in Fig. 9.

B. Layouts of Electrodes for DMRW

For $n = 10$, a simple architectural layout of electrodes with a single DMF rotary mixer with 16 electrodes is shown in the shaded region of Fig. 10. However, a more efficient architectural layout of electrodes can be obtained by using two DMF rotary mixers instead of one (Fig. 10). At the cost of hardware overhead, the design with two mixers offers more parallelism that yields faster operation and yet maintains its overall simplicity. For a 10-bit precision, the proposed layout with two $(k : k)$ DMF rotary mixers (here, $1 \leq k \leq 5$), each with 16 electrodes, is shown in Fig. 10. The locations of 18 [i.e., $2(n-1)$] storage units are shown by black dots in the figure. The droplet pathways from the two inputs, from the DMF rotary mixers (for the target output and for the waste droplets), are shown with arrow-head lines in both the layouts.

C. Storage Units

There is nothing unique in functionality of the storage electrodes compared to the normal electrodes used in the proposed layouts. A storage electrode provides a space on which the intermediate droplet can sit for later use. Any electrode in the layout can be used as a storage unit. The storage elements are allocated in such a fashion that the fluidic constraints are not violated during the droplet movements in the dilution process on-chip. Fluidic constraint rules are explained in detail in [1]. The droplet sitting on a storage electrode should not interfere with the flow-paths of the other droplets. In this way, the unintended mixing on the layout

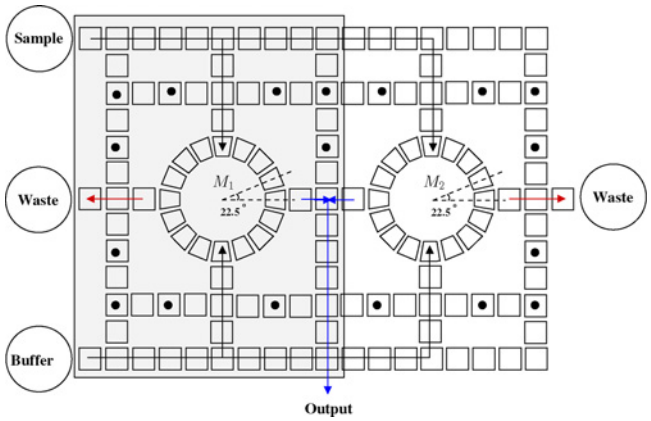

Fig. 10. Layout of electrodes with two DMF rotary mixers for $n = 10$.

TABLE III
MIXING/SPLITTING STEPS OBTAINED FROM DMRW FOR $C_t = \frac{313}{1024}$

Step	*mix_split* Operations	Resultant CF
1.	*mix_split*(0/1024, 1024/1024)	512/1024
2.	*mix_split*(0/1024, 512/1024)	256/1024
3.	*mix_split*(256/1024, 512/1024)	384/1024
4.	*mix_split*(256/1024, 384/1024)	320/1024
5.	*mix_split*(256/1024, 320/1024)	288/1024
6.	*mix_split*(288/1024, 320/1024)	304/1024
7.	*mix_split*(304/1024, 320/1024)	312/1024
8.	*mix_split*(312/1024, 320/1024)	316/1024
9.	*mix_split*(312/1024, 316/1024)	314/1024
10.	*mix_split*(312/1024, 314/1024)	313/1024

(which may be a mixing outside the DMF rotary mixers) of stored droplet with other droplets (input, output, waste, or intermediate) is avoided. Thus, to satisfy the fluidic constraints with the neighborhood electrodes, adjacent electrodes of a storage unit are kept blank, i.e., are not used for any purpose. Another important fact is that, the mixer module can itself be used as storage, while the stored droplets may be used in a subsequent mix/split step.

D. Mapping Mix/Split Steps into Layout with Two Mixers

The execution of the waste minimizing dilution algorithm DMRW on the proposed layout of Fig. 10 can be well-understood using an example. The mix/split steps determined by DMRW need to be mapped or scheduled to the mixer modules properly to achieve the efficiency of the algorithm. For example, to obtain the target concentration of $C_t = \frac{313}{1024}$ of a substance fluid, from the supply of same fluid with two CFs $C_h = \frac{1024}{1024}$ and $C_l = \frac{0}{1024}$ (i.e., buffer solution), the detailed mix/split steps obtained by DMRW are shown in Table III.

After analyzing the mix/split steps for the target CF $C_t = \frac{313}{1024}$, shown in Table III, the demands in terms of the number of unit-volume droplets of different intermediate CFs are calculated and are shown in Table IV. These droplet demands are calculated by bottom-up scanning of the mix/split steps in Table III, i.e., by backtracing the corresponding mix/split digraph. At any step of the mix/split sequence (shown in Table III), the demand of the number of unit-volume droplets of the resultant intermediate CF is calculated as follows. If the total number of unit-volume droplets of

TABLE IV
DEMAND CALCULATION IN TERMS OF NUMBER OF DROPLETS OF DIFFERENT INTERMEDIATE CFS (SHOWN WITHIN THE PARENTHESES) AND MIXER (MODULE) ASSIGNMENTS FOR $C_t = \frac{313}{1024}$

Step	Lower CF	Higher CF	Resultant CF	Mixer
10	312/1024 (1)	314/1024 (1)	313/1024 (2)	M_1
9	312/1024 (1)	316/1024 (1)	314/1024 (2)	M_1
8	312/1024 (1)	320/1024 (1)	316/1024 (2)	M_1
7	304/1024 (2)	320/1024 (2)	312/1024 (4)	M_2
6	288/1024 (1)	320/1024 (1)	304/1024 (2)	M_2
5	256/1024 (1)	320/1024 (1)	288/1024 (2)	M_2
4	256/1024 (3)	384/1024 (3)	320/1024 (6)	M_1
3	256/1024 (2)	512/1024 (2)	384/1024 (4)	M_2
2	0/1024 (3)	512/1024 (3)	256/1024 (6)	M_1
1	0/1024 (3)	1024/1024 (3)	512/1024 (6)	M_1

that resultant CF to be used in the following steps of the mix/split sequence is p, then the demand of the number of unit-volume droplets of the resultant intermediate CF is $2.\lceil \frac{p}{2} \rceil$. For example, consider the fourth step of the mix/split sequence shown in Table III. To determine the number of unit-volume droplets to be produced of the resultant CF $\frac{320}{1024}$, we determine the number of unit-volume droplets of CF $\frac{320}{1024}$ that are needed in subsequent mixing steps toward the target CF. It is observed that in the subsequent mixing steps, a total of five unit-volume droplets of intermediate $CF = \frac{320}{1024}$ will be used to generate the next resultant CFs. Thus, the demand of the resultant CF $\frac{320}{1024}$ is calculated as six. In this way, the complete mix/split sequence is scanned bottom-up to obtain the droplet demands of different intermediate CFs as shown in Table IV. The backtracing phase is also shown pictorially in Fig. 4.

During the generation of two droplets of target CF $C_t = \frac{313}{1024}$ from the two extreme concentrations $C_l = \frac{0}{1024}$ (buffer solution) and $C_h = \frac{1024}{1024}$ (100% sample), the total number of droplets of C_l and C_h required are six and three, respectively. The total number of waste droplets is seven and these are of the following concentrations: $\frac{512}{1024}$, $\frac{512}{1024}$, $\frac{384}{1024}$, $\frac{320}{1024}$, $\frac{288}{1024}$, $\frac{312}{1024}$, $\frac{316}{1024}$, and $\frac{314}{1024}$. Also, an example mixer (module) assignment is shown in the last column of Table IV for the target $CF = \frac{313}{1024}$. This example identifies the mix/split operation that are be executed in each of the two mix/split modules (M_1 or M_2) in the layout of Fig. 10. An efficient mixer (module) assignment can reduce the on-chip dilution time by avoiding additional transportation of intermediate and waste droplets in the mix/split steps while continuous emission of target droplets is needed. Thus, the proposed dilution algorithm DMRW and layout of electrodes make the dilution process fast with reduced wastage of sample or reagent and buffer solution. Together, they also provide high-throughput during the continuous emission of target droplets.

E. Tradeoff Between Hardware Resource and Dilution Time

Assume that the two dilution graphs (sequence of mix/split steps) for a target CF describing the BS method and the DMRW method, are mapped into the same chip with a single DMF rotary mixer as shown in Fig. 10. For the DMRW method, the last two intermediate CF droplets are used in subsequent mixing steps, which need to be stored on-chip. For the BS method, the current CF droplet is immediately used

in conjunction with sample or buffer. Since no intermediate droplets are stored, the dilution process may be faster since no time is required to transport intermediate droplets. Thus, for a layout with a single DMF rotary mixer, the dilution time for DMRW method may exceed that for the BS method because of transportation overhead.

With the architectural layout with two DMF rotary mixers (Fig. 10), the dilution process can be expedited by concurrent transportation of intermediate CF droplets to and from the storage units with those from the reservoirs (dispensing and moving). Thus, the mapping of mix/split steps into a layout involves a tradeoff between dilution time and number of available rotary mixers (here, two). Furthermore, with increasing number of mix/split steps, this tradeoff will be more pronounced, and consequently a befitting architecture is hard to design. However, irrespective of the layout architecture, the DMRW method always offers nonnegative savings in the number of waste droplets compared to that of the BS method.

In this context, it may be noted that with increase in hardware resources (e.g., number of mixers), on-chip dilution time may reduce up to a certain extent initially. However, droplet transportation time will increase and because of some inherent sequential nature of the dilution algorithm, it may not scale-up uniformly with addition of resources. Therefore, for all practical purposes, it is convenient to compromise dilution time against certain specific architecture with a given number of mixers and mix/split steps. Thus, the proposed layout fits well to the architectural requirement of the DMRW method.

VIII. Conclusion

We have proposed an efficient and practical method for automated dilution/mixing of samples/reagents and an architectural layout of electrodes for on-chip implementation. The method reduced wastage, which, in turn, reduced the need for large volumes of samples/reagents and buffer solutions. Since the technique always use the boundary CFs, which dynamically approach the target concentration, it reduced the loss of sample and buffer solutions. For sample dilution with error bound less than $\frac{1}{2^{10}}$, it yielded 29% average savings in both sample and buffer consumption, and 37% average savings in waste droplet emission compared to the BS technique. The scheme always provided nonnegative savings (up to 89%) in waste droplets. If in addition to balanced mixing, $(k : \ell)$ mixing is also performed in the DMF rotary mixers, where, $k \neq \ell$, then the scheme can be improved to further minimize the total number of waste droplets. Designing a dilution scheme allowing unbalanced $(k : \ell)$ mixing for further minimization of dilution time and wastage is left as an open problem.

Acknowledgment

The authors would like to thank the anonymous reviewers of the manuscript for their critical comments and valuable suggestions.

References

[1] K. Chakrabarty and F. Su, *Digital Microfluidic Biochips: Synthesis, Testing and Reconfiguration Techniques*. Boca Raton, FL: CRC Press, 2007.

[2] J. Ding, K. Chakrabarty, and R. B. Fair, "Scheduling of microfluidic operations for reconfigurable 2-D electrowetting arrays," *IEEE Trans. Comput.-Aided Des. Integr. Circuits Syst.*, vol. 20, no. 12, pp. 1463–1468, Dec. 2001.

[3] R. Sista, Z. Hua, P. Thwar, A. Sudarsan, V. Srinivasan, A. Eckhardt, M. Pollack, and V. Pamula, "Development of a digital microfluidic platform for point of care testing," *Lab. Chip*, vol. 8, no. 12, pp. 2091–2104, 2008.

[4] H. Moon, A. R. Wheeler, R. L. Garrell, J. A. Loo, and C.-J. Kim, "An integrated digital microfluidic chip for multiplexed proteomic sample preparation and analysis by MALDI-MS," *Lab. Chip*, vol. 6, no. 9, pp. 1213–1219, 2006.

[5] M. Abdelgawad and A. R. Wheeler, "The digital revolution: A new paradigm for microfluidics," *Adv. Mater.*, vol. 21, no. 8, pp. 920–925, 2009.

[6] R. B. Fair, "Digital microfluidics: Is a true lab-on-a-chip possible?" *Microfluid Nanofluid*, vol. 3, no. 3, pp. 245–281, Mar. 2007.

[7] R. B. Fair, A. Khlystov, T. D. Tailor, V. Ivanov, R. D. Evans, P. B. Griffin, V. Srinivasan, V. K. Pamula, M. G. Pollack, and J. Zhou, "Chemical and biological applications of digital-microfluidic devices," *IEEE Des. Test Comput.*, vol. 24, no. 1, pp. 10–24, Jan. 2007.

[8] V. Srinivasan, V. K. Pamula, and R. B. Fair, "An integrated digital microfluidic lab-on-a-chip for clinical diagnostics on human physiological fluids," *Lab. Chip*, vol. 4, no. 4, pp. 310–315, 2004.

[9] *Global In Vitro Diagnosis Market Analysis*. (2008, Jun.). PRLog Free Press Release [Online]. Available: http://www.prlog.org/10080477-global-in-vitro-diagnostic-market-analysis

[10] *World Malaria Day: Key Figures*. (2009, Apr.) [Online]. Available: http://www.rollbackmalaria.org/worldmalariaday/keyfigures

[11] *International Technology Roadmap for Semiconductors* [Online]. Available: http://www.itrs.net/

[12] K. F. Bohringer, "Modeling and controlling parallel tasks in droplet-based microfluidic systems," *IEEE Trans. Comput.-Aided Des. Integr. Circuits Syst.*, vol. 25, no. 2, pp. 334–344, Feb. 2006.

[13] P.-H. Yuh, C.-L. Yang, and Y.-W. Chang, "Placement of defect-tolerant digital microfluidic biochips using the T-tree formulation," *ACM J. Emerg. Technol. Comput. Syst.*, vol. 3, no. 3, pp. 1550–4832, 2007.

[14] T.-W. Huang and T.-Y. Ho, "A fast routability and performance-driven droplet routing algorithm for digital microfluidic biochips," in *Proc. ICCD*, Oct. 2009, pp. 445–450.

[15] E. Maftei, P. Pop, and J. Madsen, "Tabu search-based synthesis of dynamically reconfigurable digital microfluidic biochips," in *Proc. CASES*, Oct. 2009, pp. 195–204.

[16] P.-H. Yuh, S. Sapatnekar, C.-L. Yang, and Y.-W. Chang, "A progressive-ILP based routing algorithm for cross-referencing biochips," in *Proc. DAC*, Jun. 2008, pp. 284–289.

[17] C. C.-Y. Lin and Y.-W. Chang, "ILP-based pin-count aware design methodology for microfluidic biochips," in *Proc. DAC*, Jul. 2009, pp. 258–263.

[18] E. Maftei, P. Paul, J. Madsen, and T. K. Stidsen, "Placement-aware architectural synthesis of digital microfluidic biochips using ILP," in *Proc. VLSI-SoC*, Oct. 2008, pp. 425–430.

[19] T.-W. Huang, C.-H. Lin, and T.-Y. Ho, "A contamination aware droplet routing algorithm for digital microfluidic biochips," in *Proc. ICCAD*, Nov. 2009, pp. 151–156.

[20] P.-H. Yuh, C.-L. Yang, and Y.-W. Chang, "BioRoute: A network-flow-based routing algorithm for the synthesis of digital microfluidic biochips," *IEEE Trans. Comput.-Aided Des. Integr. Circuits Syst.*, vol. 27, no. 11, pp. 1928–1941, Nov. 2008.

[21] M. Cho and D. Z. Pan, "A high-performance droplet routing algorithm for digital microfluidic biochips," *IEEE Trans. Comput.-Aided Des. Integr. Circuits Syst.*, vol. 27, no. 10, pp. 1714–1724, Oct. 2008.

[22] Z. Xiao and E. F. Young, "CrossRouter: A droplet router for cross-referencing digital microfluidic biochips," in *Proc. ASPDAC*, 2010, pp. 269–274.

[23] T.-W. Huang and T.-Y. Ho, "A two-stage ILP-based droplet routing algorithm for pin-constrained digital microfluidic biochips," in *Proc. ACM ISPD*, Mar. 2010, pp. 201–208.

[24] C.-Y. Lin and Y.-W. Chang, "Cross contamination aware design methodology for pin-constrained digital microfludic biochips," in *Proc. DAC*, 2010, pp. 641–646.

[25] R. B. Fair, V. Srinivasan, H. Ren, P. Paik, V. K. Pamula, and M. G. Pollack, "Electrowetting-based on-chip sample processing for integrated microfluidics," in *Proc. IEEE IEDM Tech. Dig.*, 2003, pp. 32.5.1–32.5.4.

[26] H. Ren, V. Srinivasan, and R. B. Fair, "Design and testing of an interpolating mixing architecture for electrowetting-based droplet-on-chip chemical dilution," in *Proc. Int. Conf. Solid-State Sensors, Actuators Microsyst. (Tranducers)*, 2003, pp. 619–622.
[27] M. J. Jebrail and A. R. Wheeler, "Digital microfluidic method for protein extraction by precipitation," *J. Anal. Chem.*, vol. 81, no. 1, pp. 330–335, Jan. 2009.
[28] K. E. Herold and A. Rasooly, *Lab-on-a-Chip Technology (Vol. 1): Fabrication and Microfluidics*. Norfolk, U.K.: Caister Academic Press, Aug. 2009.
[29] A. T. O'Neill and G. M. Walker, "Chapter 18: Linear dilution microfluidic devices," in *Lab-on-a-Chip Technology (Vol. 1): Fabrication and Microfluidics*. Norfolk, U.K.: Caister Academic Press, Aug. 2009.
[30] C. Kim, K. Lee, J. H. Kim, K. S. Shin, K.-J. Lee, T. S. Kim, and J. Y. Kang, "A serial dilution microfluidic device using a ladder network generating logarithmic or linear concentrations," *Lab. Chip*, vol. 8, no. 3, pp. 473–479, 2008.
[31] H. A. Yusuf, S. J. Baldock, P. R. Fielden, N. J. Goddard, S. Mohr, and B. J. T. Brown, "Systematic linearisation of a microfluidic gradient network with unequal solution inlet viscosities demonstrated using glycerol," *Microfluidics Nanofluidics*, vol. 8, no. 5, pp. 587–598, 2009.
[32] K. Lee, C. Kim, G. Jung, T. S. Kim, J. Y. Kang, and K. W. Oh, "Microfluidic network-based combinatorial dilution device for high throughput screening and optimization," *Microfluidics Nanofluidics*, vol. 8, no. 5, pp. 677–685, 2009.
[33] K. Lee, C. Kim, B. Ahn, R. Panchapakesan, A. R. Full, L. Nordee, J. Y. Kang, and K. W. Oh, "Generalized serial dilution module for monotonic and arbitrary microfluidic gradient generators," *Lab. Chip*, vol. 9, no. 5, pp. 709–717, 2009.
[34] E. J. Griffith, S. Akella, and M. K. Goldberg, "Performance characterization of a reconfigurable planar-array digital microfluidic system," *IEEE Trans. Comput.-Aided Des. Integr. Circuits Syst.*, vol. 25, no. 2, pp. 345–357, Feb. 2006.
[35] J. P. Urbanski, W. Thies, C. Rhodes, S. Amarasinghe, and T. Thorsen, "Digital microfluidics using soft lithography," *Lab. Chip*, vol. 6, no. 1, pp. 96–104, 2006.
[36] W. Thies, J. P. Urbanski, T. Thorsen, and S. Amarasinghe, "Abstraction layers for scalable microfluidic biocomputing," *Nat. Comput.*, vol. 7, no. 2, pp. 255–275, May 2008.
[37] M. G. Pollack, R. B. Fair, and A. D. Shenderov, "Electrowetting-based actuation of liquid droplets for microfluidic applications," *Appl. Phys. Lett.*, vol. 77, no. 11, pp. 1725–1726, 2000.
[38] E. Miller and A. R. Wheeler, "Digital bioanalysis," *Anal. Bioanal. Chem.*, vol. 393, no. 2, pp. 419–426, Jan. 2009.
[39] F. Su, W. Hwang, and K. Chakrabarty, "Droplet routing in the synthesis of digital microfluidic biochips," in *Proc. DATE*, 2006, pp. 323–328.
[40] S. K. Cho, H. Moon, and C.-J. Kim, "Creating, transporting, cutting, and merging liquid droplets by electrowetting-based actuation for digital microfluidic circuits," *J. Microelectromechanic. Syst.*, vol. 12, no. 1, pp. 70–80, Feb. 2003.
[41] Y. Fouillet, D. Jary, C. Chabrol, P. Claustre, and C. Peponnet, "Digital microfluidic design and optimization of classic and new fluidic functions for lab on a chip systems," *Microfluidics Nanofluidics*, vol. 4, no. 3, pp. 159–165, Mar. 2008.
[42] T. Xu, V. K. Pamula, and K. Chakrabarty, "Automated, accurate and inexpensive solution-preparation on a digital microfluidic biochip," in *Proc. IEEE BIOCAS*, Nov. 2008, pp. 301–304.
[43] T. Xu, K. Chakrabarty, and V. K. Pamula, "Design and optimization of a digital microfluidic biochip for protein crystallization," in *Proc. ICCAD*, 2008, pp. 297–301.
[44] Duke University Digital Microfluidics Laboratory, *Ring Structure: Digital Microfluidics by Electrowetting* (2009, Sep.) [Online]. Available: http://microfluidics.ee.duke.edu/videos/mpegs/rotary_flow.mpg

Sudip Roy (S'09) received the B.Sc. (Hons.) degree in physics and the B.Tech. degree in computer science and engineering from the University of Calcutta, Kolkata, India, in 2001 and 2004, respectively, and the M.S. degree in computer science and engineering from the Indian Institute of Technology Kharagpur, Kharagpur, India, in 2009. He is currently pursuing the Ph.D. degree in computer science and engineering from the Indian Institute of Technology Kharagpur.

His current research interests include algorithms for computer-aided design and testing of digital very-large-scale integration circuits and digital microfluidic biochips.

Mr. Roy was a recipient of the Microsoft India Research Ph.D. Fellowship Award in 2010.

Bhargab B. Bhattacharya (F'07) received the B.Sc. (Hons.) degree in physics, the B.Tech. and M.Tech. degrees in radiophysics and electronics, and the Ph.D. degree in computer science, all from the University of Calcutta, Kolkata, India.

He is currently a Professor with the Advanced Computing and Microelectronics Unit, Indian Statistical Institute, Kolkata, India. He was a Visiting Professor with the University of Nebraska, Lincoln, and with the University of Potsdam, Potsdam, Germany. In 2005, he visited the Indian Institute of Technology Kharagpur, Kharagpur, India, as a VSNL Chair Professor. His current research interests include VLSI design and testing, digital geometry, image processing architecture, and computational nanoscience. He has authored more than 220 papers in archival journals and in peer-reviewed conference proceedings, and holds nine U.S. patents.

Dr. Bhattacharya is currently serving on the Editorial Board of the *Journal of Electronic Testing: Theory and Applications* (Springer). He is a Fellow of the Indian National Academy of Engineering and the National Academy of Sciences, India. He was a recipient of the TechnoMentor Award of the India Semiconductor Association in 2008.

Krishnendu Chakrabarty (F'08) received the B. Tech. degree from the Indian Institute of Technology Kharagpur, Kharagpur, India, in 1990, and the M.S.E. and Ph.D. degrees from the University of Michigan, Ann Arbor, in 1992 and 1995, respectively.

He is currently a Professor with the Department of Electrical and Computer Engineering, Duke University, Durham, NC, and is a member of the Chair Professor Group (honorary position) in Software Theory with the School of Software, Tsinghua University, Beijing, China. His current research interests include testing and design-for-testability of integrated circuits, digital microfluidics and biochips, circuits, and systems based on DNA self-assembly, and wireless sensor networks. He has authored nine books on these topics, contributed nearly 20 chapters to book volumes, published over 340 papers in journals and refereed conference proceedings, and given over 130 invited, keynote, and plenary talks.

Prof. Chakrabarty is a Golden Core Member of the IEEE Computer Society, and a Distinguished Engineer of Association for Computing Machinery (ACM). He was an Invitational Fellow of the Japan Society for the Promotion of Science in 2009. He served as a Distinguished Visitor of the IEEE Computer Society from 2005 to 2007, and as a Distinguished Lecturer of the IEEE Circuits and Systems Society from 2006 to 2007. Currently, he serves as an ACM Distinguished Speaker, as well as a Distinguished Visitor of the IEEE Computer Society for 2010 to 2012. He is the Editor-in-Chief for the IEEE DESIGN AND TEST OF COMPUTERS and for the *ACM Journal on Emerging Technologies in Computing Systems*. He is an Associate Editor of the IEEE TRANSACTIONS ON COMPUTER-AIDED DESIGN OF INTEGRATED CIRCUITS AND SYSTEMS, IEEE TRANSACTIONS ON CIRCUITS AND SYSTEMS II, and IEEE TRANSACTIONS ON BIOMEDICAL CIRCUITS AND SYSTEMS. He serves as an Editor of the *Journal of Electronic Testing: Theory and Applications*. He is a recipient of the Duke University Graduate School Dean's Award for Excellence in Mentoring in 2008, and the Capers and Marion McDonald Award for Excellence in Mentoring and Advising, Pratt School of Engineering, Duke University, in 2010. He is a recipient of the National Science Foundation Early Faculty (Career) Award, the Office of Naval Research Young Investigator Award, the Humboldt Research Fellowship from the Alexander von Humboldt Foundation, Germany, and several Best Papers Awards at IEEE conferences.